

## Supporting Information

### **Pronounced Effect of Strain Biaxiality on High-Temperature Behavior of Strain-Crystallizing Elastomers†**

Ryosuke Osumi,<sup>a</sup> Thanh-Tam Mai,<sup>b</sup> Katsuhiko Tsunoda,<sup>c</sup> Kenji Urayama<sup>b,\*</sup>

<sup>a</sup> Department of Polymer Science and Engineering, Kyoto Institute of Technology, Matsugasaki, Sakyo-ku, Kyoto 606-8585, Japan

<sup>b</sup> Department of Material Chemistry, Kyoto University, Nishikyo-ku, Kyoto 615-8510, Japan

<sup>c</sup> Sustainable and Advanced Materials Division, Bridgestone Corporation, Tokyo 187-8531, Japan

\*To whom correspondence should be addressed: [urayama.kenji.2s@kyoto-u.ac.jp](mailto:urayama.kenji.2s@kyoto-u.ac.jp)

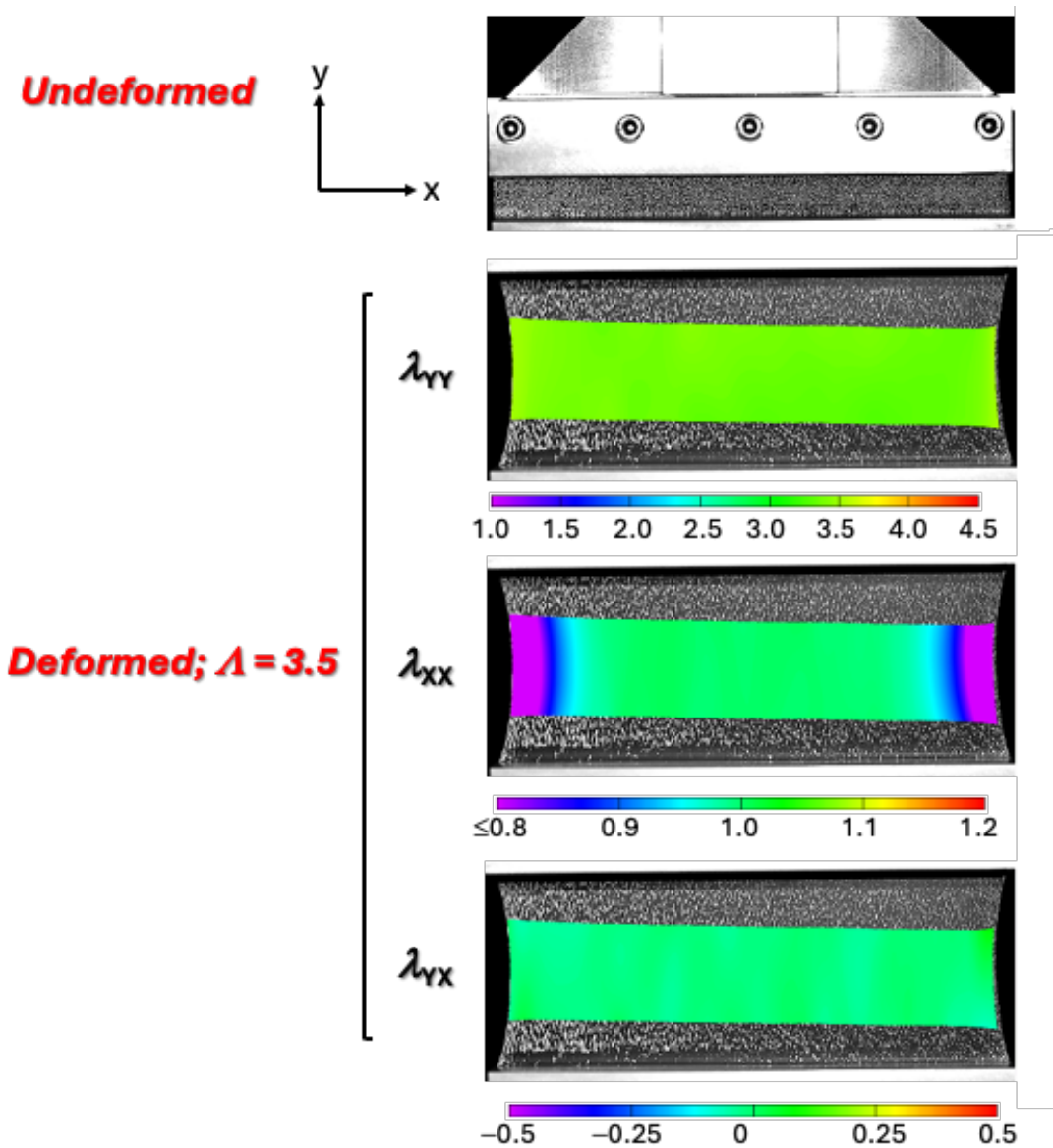


**Fig. S1.** Spatial distribution of each component in deformation gradient tensor in the P-geometry under an applied stretch of  $\Lambda_y = 3.5$ . In the observed region,  $\lambda_{yy}$  is uniform while  $\lambda_{yx}$  is nearly zero, indicating negligible shear. The variations in  $\lambda_{yy}$  indicate the transition of local deformation from planar to pseudo-uniaxial stretching as the position shifts from the center to free edges.

## S-2. Crystallinity Evaluation via Surface Calorimetry

### S-2-1. Outline

This section describes the outline of the method for evaluating the crystallinity from heat emission observed during stretching of NR samples in the U- and P-geometries (Fig. 1). This evaluation follows the methodology established by Le Cam et al. which determines crystallinity from heat emission in a rectangular NR specimen under uniform uniaxial stretching.<sup>1,2</sup> Temperature rises ( $\Delta T$ ) measured during stretching under nonadiabatic conditions are influenced by thermal dissipation and other factors. The following heat diffusion model combining heat generation and dissipation<sup>3</sup> was utilized:

$$s = \rho C \left( \frac{dT}{dt} + \frac{\Delta T}{\tau} \right) \quad (\text{S2} - 1)$$

where  $s$  is the overall heat power density caused by applied deformation,  $t$  is the elapsed time after deformation onset,  $\rho$  ( $= 0.936 \text{ kg/dm}^3$ ) and  $C$  ( $= 1768 \text{ J/kg}\cdot\text{K}$ ) are the sample density and the heat capacity, respectively. The time constant for heat dissipation at the position of interest ( $\tau$ ) was separately estimated from the temperature recovery, as described in next section. The  $\Delta T$ - $A_y$  data obtained at each position (**Figure S2a**) were converted into the  $s$ - $A_y$  relationships using equation (S1) (**Figure S2b**). The applied stretch ( $A_y$ ) is a function of  $t$  as expressed by  $A_y = (L_{y0} + Vt)/L_{y0}$  where  $L_{y0}$  and  $V$  are the initial gauge length and crosshead speed, respectively. The overall heat power density ( $s$ ) beyond the onset stretch of SIC ( $A_y > A_y^*$ ) contains contributions from SIC ( $s_{\text{SIC}}$ ) and entropy elasticity (Gough-Joule effect) ( $s_{\text{GJ}}$ ). By fitting an empirical function to the data at  $A_y < A_y^*$  without SIC (**Figure S2b**, black line),  $s_{\text{GJ}}$  was extrapolated to higher  $A_y$ , enabling the evaluation of  $s_{\text{SIC}}$  at  $A_y > A_y^*$ . The  $s$ - $A_y$  data at each position were used for evaluating  $s_{\text{GJ}}$ . The temperature rise specifically stemming from SIC as a function of  $t$  (or  $A_y$ ) (**Figure S2c**) was estimated as:

$$\Delta T_{\text{SIC}}(t) = \frac{s_{\text{SIC}}(t)\Delta t}{\rho C} + \Delta T_{\text{SIC}}(t - \Delta t) \quad (\text{S2} - 2)$$

where  $\Delta T_{\text{SIC}}(0) = 0$ . Crystallinity  $\chi(t)$  [or  $\chi(A_y)$ ] (**Figure S2d**) was calculated from:

$$\chi(t) = \frac{\rho C \Delta T_{\text{SIC}}(t)}{\Delta H} \quad (\text{S2} - 3)$$

with  $\Delta H$  ( $= 6.2 \times 10^4 \text{ J/dm}^3$ ), the equilibrium enthalpy of melting of polyisoprene crystal.<sup>4</sup> For the U-geometry, this protocol was applied to the  $\Delta T$ - $A_y$  data at the central position of the samples. For the P-geometry, this protocol was applied to the data at selected 10 positions along the central horizontal line (**Figure 3e**). **Figure S3** shows the results via this protocol for the central position in the P-geometry of the NR specimen.

At low values of  $A_y$ , below the threshold for SIC initiation, the calculated  $s_{\text{SIC}}$  values obtained by subtracting the estimated  $s_{\text{GJ}}$  from the total  $s$  should ideally be zero. However, due to inherent scatter in the raw  $s$  data,  $s_{\text{SIC}}$  occasionally appears slightly negative (although its level is extremely close to zero). Since such negative  $s_{\text{SIC}}$  values are physically meaningless (implying negative  $\chi$ ), they were set to zero in the analysis.

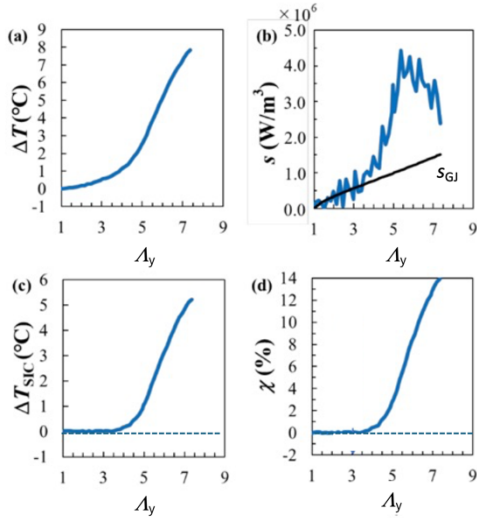


**Fig. S2.** (a)  $\Delta T$ , (b)  $s$ , (c)  $\Delta T_{\text{SIC}}$  and (d)  $\chi$  as a function of  $A_y$  for a NR specimen in the U-geometry stretching. The data are obtained at the central position of the specimen.

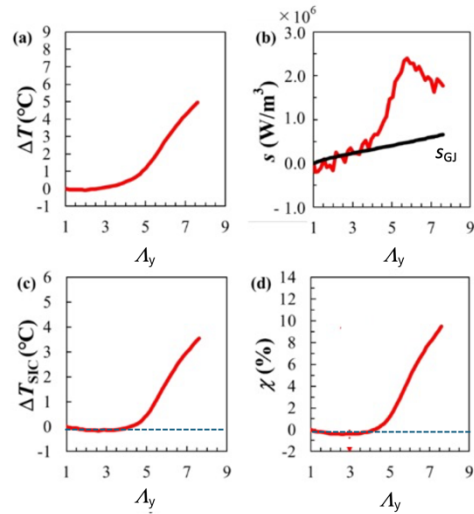


**Fig. S3.** (a)  $\Delta T$ , (b)  $s$ , (c)  $\Delta T_{\text{SIC}}$  and (d)  $\chi$  as a function of  $A_y$  for a NR specimen in the P-geometry stretching. The data are obtained at the central position of the specimen.

## S2-2. Evaluation of time constant for heat dissipation

Local time constant for heat dissipation at the position of interest ( $\tau$ ) was evaluated from temperature recovery to ambient temperature following the SIC-driven temperature rise (**Figure S4**). This temperature recovery was measured for specimens stretched rapidly to  $A_y = 7$  at a crosshead speed of 15 mm/s. The  $\tau$  value was evaluated by fitting a single exponential function.

We also considered the local strain dependence of  $\tau$ , which originates from thickness reductions during stretching, according to the method of Le Cam et al.<sup>1,2</sup> This effect was considered using the deformation biaxiality ratio as:

$$\tau = \frac{\tau_0}{\lambda_x \lambda_y} \quad (\text{S2} - 4)$$

where  $\tau_0$  is the dissipation time constant in the undeformed state. The time  $\tau_0$  at each position was obtained using the values of  $\lambda_x$ ,  $\lambda_y$  and  $\tau$  at  $A_y = 7$ .

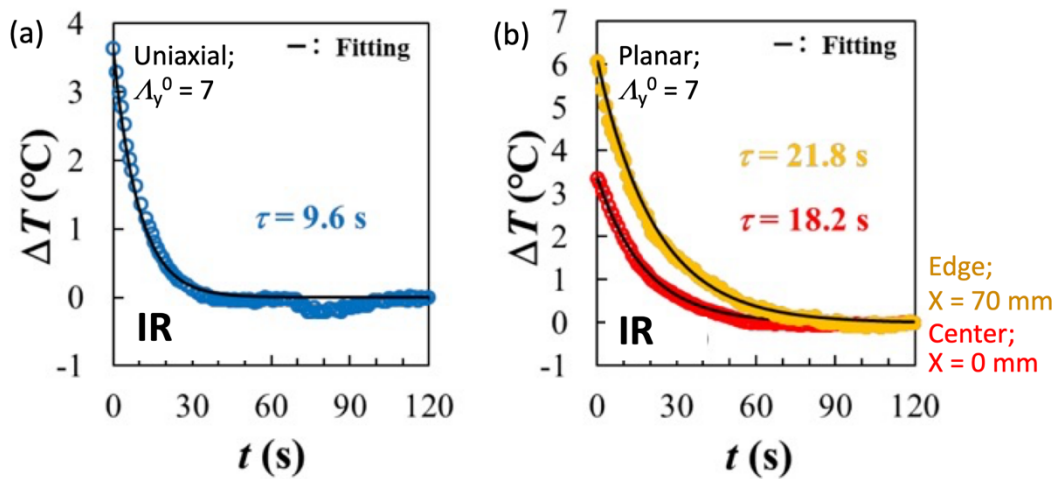


**Fig. S4.** Recovery behavior after temperature rise via SIC driven by applied rapid and constant stretch ( $A_{y0}$ ) for the IR specimens at (a) the central position in the U-geometry and (b) the central and edge positions in the P-geometry. The black lines in the figures represent the fitted single exponential functions with the characteristic times ( $\tau$ ).

### References:

- (1) Le Cam, J.-B. Strain-Induced Crystallization in Rubber: A New Measurement Technique. *Strain* **2018**, 54 (1), e12256.
- (2) Le Cam, J.-B.; Albouy, P.-A.; Charlès, S. Comparison between X-Ray Diffraction and Quantitative Surface Calorimetry Based on Infrared Thermography to Evaluate Strain-Induced Crystallinity in Natural Rubber. *Revi Sci Instrum* **2020**, 91 (4), 044902.
- (3) Chrysochoos, A. Analyse Du Comportement Des Matériaux Par Thermographie Infra Rouge. *Colloque Photomécanique* **1995**, 95, 201–211.
- (4) Kim, H.; Mandelkern, L. Multiple Melting Transitions in Natural Rubber. *Journal of Polymer Science Part A-2: Polymer Physics* **1972**, 10 (6), 1125–1133.